MOLECULAR AND CELLULAR BIOLOGY, Mar. 2004, p. 2181–2189 Vol. 24, No. 5
0270-7306/04/$08.00+0 DOI: 10.1128/MCB.24.5.2181–2189.2004

Control of Cyclin G2 mRNA Expression by Forkhead Transcription Factors: Novel Mechanism for Cell Cycle Control by Phosphoinositide 3-Kinase and Forkhead

Lorena Martínez-Gac,[1] Miriam Marqués,[1] Zaira García,[1] Miguel R. Campanero,[2] and Ana C. Carrera[1]*

Department of Immunology and Oncology, Centro Nacional de Biotecnología/CSIC, Universidad Autónoma de Madrid, Cantoblanco, Madrid E-28049,[1] and Instituto de Investigaciones Biomédicas Alberto Sols, Madrid E-28029,[2] Spain

Received 21 July 2003/Returned for modification 29 August 2003/Accepted 4 December 2003

Cyclin G2 is an unconventional cyclin highly expressed in postmitotic cells. Unlike classical cyclins that promote cell cycle progression, cyclin G2 blocks cell cycle entry. Here we studied the mechanisms that regulate cyclin G2 mRNA expression during the cell cycle. Analysis of synchronized NIH 3T3 cell cultures showed elevated cyclin G2 mRNA expression levels at G_0, with a considerable reduction as cells enter cell cycle. Downregulation of cyclin G2 mRNA levels requires activation of phosphoinositide 3-kinase, suggesting that this enzyme controls cyclin G2 mRNA expression. Because the phosphoinositide 3-kinase pathway inhibits the FoxO family of forkhead transcription factors, we examined the involvement of these factors in the regulation of cyclin G2 expression. We show that active forms of the forkhead transcription factor FoxO3a (FKHRL1) increase cyclin G2 mRNA levels. Cyclin G2 has forkhead consensus motifs in its promoter, which are transactivated by constitutive active FoxO3a forms. Finally, interference with forkhead-mediated transcription by overexpression of an inactive form decreases cyclin G2 mRNA expression levels. These results show that FoxO genes regulate cyclin G2 expression, illustrating a new role for phosphoinositide 3-kinase and FoxO transcription factors in the control of cell cycle entry.

Symmetrical cell division is the process by which a cell duplicates its DNA content and cell mass to produce two daughter cells (42, 46, 49, 58, 60). Progression through the cell cycle is mediated by activation of the cyclin-dependent protein kinases (Cdks) (43). Cdk activation requires its binding to a specific regulatory subunit, termed cyclin. Cyclins are collectively defined by the cyclin box, a highly conserved motif that consists of approximately 100 amino acids and is essential for association with Cdk (38, 39). Cyclin-Cdk complexes are universal cell cycle regulators, with each complex controlling transition between different cell cycle phases by phosphorylation of specific substrates (35). In addition, cyclin-Cdk pairs participate in processes not directly related to cell cycle regulation (15, 32, 40).

Mammalian cyclins are classified into 12 different types—cyclins A to I (21, 33, 37, 44)—based on structural similarity, functional period in the cell division cycle, and regulated expression (22, 43, 51). Three G-type cyclins have been identified: cyclins G1 (57), G2 (21), and I (37). All three are expressed in terminally differentiated cells (20, 21, 37, 57). The overall expression profile of the G-type cyclins is atypical and is not associated with promotion of cell proliferation, but suggests that they act as cell cycle inhibitors in certain cell types and may contribute in inducing cell cycle arrest (3). Whereas cyclin G1 probably acts as a negative regulator of the G_2/M transition (24, 53), increased cyclin G2 expression inhibits cell cycle progression and may contribute to maintaining the quiescent state of differentiated cells (3, 20). Cyclin G2 is similar to cyclin A in the cyclin box, although no kinase activity is detected in cyclin G2 immunoprecipitates (3). Cyclins G1 and G2 can associate with the protein phosphatase PP2A (3, 41), suggesting that cyclin G-PP2A complexes inhibit cell cycle progression by altering PP2A targeting or substrate specificity.

The FoxO subfamily of forkhead transcription factors (TFs) comprises three functionally related proteins, FKHR, FKHRL1, and AFX, recently renamed FoxO1a, FoxO3a, and FoxO4, respectively (27). Forkhead TFs bind as monomers to consensus DNA-binding sequences (18). FoxO TFs upregulate expression of a variety of genes, including the CDK inhibitor $p27^{kip}$ (34); the Rb family-related protein p130 (31); proapoptotic targets, such as Bim (14) and FasL (6); and proteins that regulate G_2/M progression, such as cyclin B and Plk (2). They also downregulate expression of other genes, such as those coding for cyclins D1 and D2 (50). FoxO TF activity is regulated in vivo by the phosphatidylinositol-3-kinase (PI3K)-protein kinase B (PKB) pathway (2).

PI3K is an enzyme that transfers phosphate groups to the 3 position of the inositol ring of membrane phosphoinositides. Class IA PI3K is a heterodimer composed of a p85 regulatory subunit and a p110 catalytic subunit. Following growth factor receptor stimulation, PI3K mediates an increase in 3-polyphosphoinositides, which in turn activate downstream effectors such as PKB (2, 17, 55, 59, 63). The PI3K-PKB pathway regulates a variety of cell responses, including survival and division (17, 55, 59, 63). One consequence of PI3K-PKB activation in mammals is the negative regulation of FoxO TFs, mediated by direct PKB phosphorylation of FoxO TFs (4, 7, 11, 19, 29, 30, 34, 47). When PKB is inactive, FoxO TFs are dephospho-

* Corresponding author. Mailing address: Department of Immunology and Oncology, Centro Nacional de Biotecnología/CSIC, Carretera de Colmenar Km 15, Cantoblanco, Madrid E-28049, Spain. Phone: (34) 91/585-4846. Fax: (34) 91/372-0493. E-mail: acarrera@cnb.uam.es.

rylated and localized in the nucleus, where they can activate transcription. In contrast, PI3K-PKB activation promotes FoxO TF phosphorylation and exit from the nucleus, which results in FoxO TF inactivation (4, 6, 7, 11, 19, 30, 47).

Several studies show that cyclin G2 is a ubiquitous cell cycle regulator (21), whose expression inhibits G_1/S-phase transition (3, 21). Cyclin G2 mRNA levels fluctuate throughout the cell cycle in lymphocytes (20, 21); nonetheless, the mechanism by which cyclin G2 expression is regulated during the cell cycle is presently unknown. Here we show that cyclin G2 mRNA levels also vary during the cell cycle in fibroblasts, with a PI3K-dependent decrease during the G_1 phase. We postulated that PI3K may reduce cyclin G2 mRNA synthesis by inhibiting FoxO TF activity. The results show that FoxO genes regulate transcription of the cell cycle inhibitor cyclin G2, suggesting a new role for the PI3K-FoxO pathway in the control of the G_0/G_1 cell cycle entry.

MATERIALS AND METHODS

cDNA and reagents. The plasmid encoding an inactive form of AFX (FoxO4) (pMT2HA-ΔDB AFX) has been described previously (29). The plasmids encoding FKHRL1 (FoxO3a) (PECE-HA-FKHRL1-wt and PECE-HA-FKHRL1A3) and the pGL3-based Fas ligand promoter construct containing FoxO consensus binding sites (FHRE-Luc reporter, FasLp) were kindly donated by M. E. Greenberg (6). The pGL3-based pHX-Luc vector including the human myc promoter (Mycp) was a kind gift of K. Sugamura (56). The murine cyclin G2 promoter regions containing FoxO consensus motifs were obtained by PCR: position 986 of the murine cyclin G2 gene AF079877 (forward, 5′-TCATTTCGGAGAGGC TAGCTG-3′) and position 1337 of the murine cyclin G2 gene (reverse, 5′-AT ATCTAATAAGTGTGCTTCTAG-3′). PCR bands were subcloned into the pGL3 promoter vector (Promega), generating the cyclin G2-promoter-pGL3 vector (cycG2p). The following mouse monoclonal antibodies were used: anti-hemagglutinin (HA) (Babco), anti-$p27^{kip}$ (Pharmingen), and anti-α-tubulin (Oncogene). Anti-PKB goat polyclonal antibody was obtained from Santa Cruz. The following rabbit polyclonal antibodies were used: anti-FoxO3a (anti-FKHR, Upstate Biotechnology), anti-DP1 A33 (8), anti-p130 (Sta Cruz), anti-cyclin D3 (Transduction Laboratories), and anti-phosphoSer473-PKB (Cell Signaling). p110-CAAX was described previously (25, 26).

Cell culture and transfection. NIH 3T3 cells were cultured (37°C, 5% CO_2) in Dulbecco's modified Eagle medium supplemented with 10% heat-inactivated fetal calf serum (GIBCO), 2 mM L-glutamine, 10 mM HEPES, 100-U/ml penicillin G sodium, and 100-μg/ml streptomycin sulfate. For transfections, NIH 3T3 cells were seeded onto 150-mm-diameter dishes (4.5×10^6 cells per dish) and transfected the following day with 10 μg of the following cDNAs: empty vector (PECE), HA-FKHRL1-wt, HA-FKHRL1-A3, HA-AFX-wt, HA-AFX-A3, HA-ΔDBAFX, or p110-CAAX (2). Transient transfections were performed with Lipofectamine Plus (Gibco-BRL). After 8 h in complete medium, cells were incubated without serum (18 to 20 h) and collected or were stimulated for 3 h with 10% fetal calf serum (FCS)-supplemented medium and collected. In some assays, cells were stimulated for 3 h with 15-ng/ml platelet-derived growth factor (PDGF)-BB (Upstate Biotechnology), 20-ng/ml insulinlike growth factor 1 (IGF-1; Pharmacia), 100 μM egg yolk phosphatidic acid (PA; Sigma), or 10-ng/ml 1-oleoyl-2-hydroxy-sn-glycero-3-phosphate sodium salt lysophosphatidic acid (LPA; Avanti). In some cases, cells were preincubated with PI3K inhibitor (10 μM LY294002; Calbiochem) or MEK inhibitor (2 μM PD98059; Calbiochem) for 1 h prior to stimulation.

Cell cycle analysis and arrest. For time course studies, cells were synchronized by growth to confluence, maintained confluent for 48 h, and then released by low-density replating (1:3) in medium containing 10% FCS, collected at different time points, and examined. Alternatively, cells were arrested in distinct cell cycle phases. For G_0 arrest, cells were serum starved (18 to 20 h) in medium containing 0.1% bovine serum albumin (BSA), yielding approximately 80 to 90% of cells in the G_0/G_1 phase, according to DNA content. To obtain cells in the early G_1 phase, cells depleted of serum for 18 to 20 h were incubated in medium with 10% FCS for brief periods of 1 to 3 h, as indicated. For G_2 arrest, cells were incubated for 22 h with 5 μM etoposide (Sigma), yielding approximately 70 to 80% of cells in G_2. For M-phase arrest, cells were incubated for 22 h with 0.1-μg/ml Colcemid (GIBCO), yielding approximately 80% of cells in the M phase.

Western blotting, luciferase assays, ChIP, and immunofluorescence. Western blotting, luciferase, immunofluorescence with anti-FKHRL1 antibody (Upstate Biotechnology), and chromatin immunoprecipitation (ChIP) assays were performed as described previously (2, 5, 6, 25). For ChIP assays, immunoprecipitation was performed with anti-FKHRL1 antibody (Upstate Biotechnology) or normal rabbit serum. The DNA recovered was analyzed by PCR using the following appropriate primers: for the cyclin G2 promoter, forward primer 5′-ATTCATGAAGGCTCTAAGTTA-3′ and reverse primer 5′-GTTATTAAGCT GACACCTCTC-3′; for the cyclin D3 promoter, forward primer 5′-GCCCTCT GTCTTCAAAGTG-3′ and reverse primer 5′-TAAGGTCACTGTCTGCTTC-3′.

Northern blotting and quantitative PCR analysis. Total RNA was isolated from 5×10^6 to 10×10^6 cells by the guanidine isothiocyanate method with the RNeasy Mini kit (Qiagen). Total RNA (10 μg) was separated by electrophoresis in denaturing formaldehyde–1% agarose gels and transferred overnight to a nylon membrane (Zeta-Probe; Bio-Rad). After UV cross-linking, RNA quality and transfer efficiency were determined by methylene blue staining (36). The probes were [^{32}P]dCTP labeled by random priming with the Prime-It II random primer labeling kit (Stratagene). Hybridization was performed with ExpressHyb hybridization solution (BD Biosciences) (2 h at 68°C) in the presence of 10-μg/ml sheared salmon sperm DNA (Sigma). The membrane was washed three times in 2× SSC (150 mM sodium chloride, 15 mM sodium citrate [pH 7.0]) with 0.05% sodium dodecyl sulfate (SDS) at room temperature and once in 0.1× SSC plus 0.1% SDS at 52°C. Murine cyclin G2 probe (0.57 kb) was generated by reverse transcription-PCR (RT-PCR). For $p27^{kip}$, the probe was generated by *Eco*RI-*Hin*dIII digestion of the EXlox-mp27-FL vector encoding murine $p27^{kip}$ (45). The oligonucleotide 5′-ACGGGAGGTTTCTGTCCTCCC-3′, complementary to human 28S rRNA nucleotides 4205 to 4225, was used for loading control hybridizations. The hybridization and washing conditions were as described previously (36). PhosphorImaging (Molecular Dynamics) exposure of Northern blot filters was done routinely immediately prior to autoradiography.

Endogenous cyclin G2 mRNA expression levels were also determined by RT of total RNA, followed by real-time quantitative PCR analysis (Q-PCR). Total RNA (4 μg) was reverse transcribed by extension of random hexamer primers with Superscript II reverse transcriptase (Life Technology) according to the manufacturer's protocol. For Q-PCR, oligonucleotide primers for the cyclin G2 sequence (GenBank accession no. NM_007635) were designed to amplify a 93-bp DNA fragment. The cyclin G2 forward primer spans nucleotides 177 to 192 (5′-CCGGTCCGTGACGCC-3′), and the cyclin G2 reverse primer spans nucleotides 247 to 270 (5′-AGTTCAACAATCCGAAAAGCTGA-3′). The β-actin gene was used as a loading control (GenBank accession no. NM_007393). The sequence of the forward primer spans nucleotides 337 to 357 (5′-GGCACCAC ACCTTCTACAATG-3′), and that of the reverse primer spans nucleotides 468 to 490 (5′-TGGATGGCTACGTACATGGCTG-3′), amplifying a 153-bp product. Primers were designed with Primer Express software (PE Applied Biosystems). Amplification was performed with the ABI PRISM 7700 (PE Applied Biosystems). For each condition, the amount of cyclin G2 relative to that of actin was estimated according to the cycle threshold (Ct), which defines the PCR cycle number at which the PCR signal reaches a defined value. The relative amount of cyclin G2 was estimated as increment in Ct that represents Ct differences between cyclin G2 and actin according to the formula $\Delta Ct_{\text{cyclin G2}} = Ct_{\text{cyclin G2}} - Ct_{\text{actin}}$. After amplification of the cyclin G2 sequence, the melting curves of PCR products were acquired by stepwise temperature increase from 55°C to 95°C for 20 min. Data were analyzed with Dissociation Curves 1.0f. software (PE Applied Biosystems).

Electrophoretic mobility shift assays. Electrophoretic mobility shift assays were performed with the following double-stranded oligonucleotides: FoxO-cyclin G2 (5′-ATAGAAAGTAAAACAAACAAACAAACAAAAC-3′ and 5′-GTTTTGTTTGTTTGTTTGTTTTACTTTCTAT-3′) and FoxO-consensus (61) (5′-CTAGATGGTAAACAACTGTGACTAGTAGAACACGG-3′ and 5′-CCGTGTTCTACTAGTCACAGTTGTTTACCATCTAG-3′). Oligonucleotides were synthesized by Genotech. Complementary oligonucleotides were mixed at an equimolar ratio in 10 mM Tris (pH 7.5)–50 mM NaCl, heated to 65°C, and annealed by slow cooling to room temperature. Double-stranded oligonucleotides (200 ng) were labeled by T4 polynucleotide kinase reaction (New England Biolabs). For binding reactions, the following components were mixed and preincubated (20 min at room temperature): 3 μl (10 to 15 μg) of nuclear extract, 7 μl of buffer D (20 mM HEPES [pH 7.9], 20% glycerol, 0.1 M KCl, 0.2 mM EDTA, 0.5 mM dithiothreitol), 2 μl (20 μg) of purified BSA (New England Biolabs), 0.4 μl (2 μg) of sheared salmon sperm DNA, and 11 μl of H_2O. Unlabeled oligonucleotide competitors (200 ng) and either 15 μg of anti-FKHRL1 antibody (Upstate Biotechology) or 5 μl of rabbit polyclonal anti-DP1 antibody (8) were added to the initial mixture

prior to the preincubation step. After preincubation, labeled oligonucleotides were added (2 ng), and the mixtures were incubated (20 min at room temperature). Samples were then loaded onto a nondenaturing 4% acrylamide–0.1% bisacrylamide gel in 0.5% TBE (45 mM Tris base, 32.3 mM boric acid, 1.25 mM EDTA [pH 8.3]) at room temperature. Retarded complexes were visualized by autoradiography (16 h at room temperature).

RESULTS

Cyclin G2 mRNA expression levels vary during the fibroblast cell cycle. Cyclin G2 mRNA levels fluctuate throughout the cell cycle in lymphocytes (20, 21), but the mechanism that controls cyclin G2 expression is unknown. We first examined whether cyclin G2 mRNA expression also varies during the cell cycle in fibroblasts. To examine cell cycle progression, NIH 3T3 cells were arrested by growth to confluence and then released by low-density replating in serum-containing medium for different time periods. Figure 1A illustrates the cell cycle profiles at 0, 18, and 23 h after release, when a significant proportion of the cells are in the G_0/G_1 (0 h), S (18 h), or G_2/M (23 h) phases. Because the G_0 and G_1 phases are indistinguishable by DNA content analysis, to discriminate between them, we examined cyclin D3 levels, which increase in G_1 (22, 51); p130 levels, which decrease in G_1 (54); and PKB activation (using anti-phospho Ser473-PKB antibody), which is induced rapidly following G_1 entry (2). According to the PKB activation profiles, cyclin D3 levels, and p130 expression, confluent cells exhibit a G_0 phenotype (Fig. 1B). This was confirmed by examining intracellular FoxO TF localization, which is nuclear in G_0 (2, 31), and $p27^{kip}$ expression, which is high in G_0 (33) (data not shown). We then examined cyclin G2 mRNA expression, which was high prior to release (in quiescent cells) and decreased as cells entered the cell cycle (in G_1), increasing again at 18 to 20 h after release, corresponding to the late S and G_2/M phases (Fig. 1C).

We also examined cells arrested at different cell cycle phases. For G_0 arrest, cells were incubated in serum-deprived medium for 18 to 20 h, after which approximately 90% of the cells were in G_0/G_1, according to DNA content-based cell cycle profiles (data not shown). To distinguish between the G_0 and G_1 phases, we examined the subcellular localization of the FoxO TF FKHRL1, which is nuclear in G_0 (2, 31). FKHRL1 was localized in the nuclei in serum-deprived cells (>90% of the cells) and translocated to the cytosol following serum addition (>90% of the cells) (Fig. 1D). We also examined cyclin D3 levels (not shown), p130 protein levels, and activation of PKB (as described above) (Fig. 1E), which confirmed the quiescent state of serum-deprived cells. We also examined cells arrested in the G_2 and M phases (see Materials and Methods). We then examined cyclin G2 mRNA expression. Cyclin G2 levels were high in serum-starved NIH 3T3 cells, decreased following serum addition, and were elevated in G_2-arrested cells, with intermediate expression in M-arrested cells (Fig. 1F). Mouse embryonic fibroblast cells, like NIH 3T3 cells, showed high cyclin G2 mRNA expression levels in G_0, which decreased following serum addition (data not shown).

Cyclin G2 mRNA downregulation requires PI3K-derived signals. To examine the signals involved in cyclin G2 mRNA downregulation during cell cycle entry, cells were arrested in G_0 by serum deprivation and released by using distinct stimuli. Cells were incubated with medium containing serum or LPA,

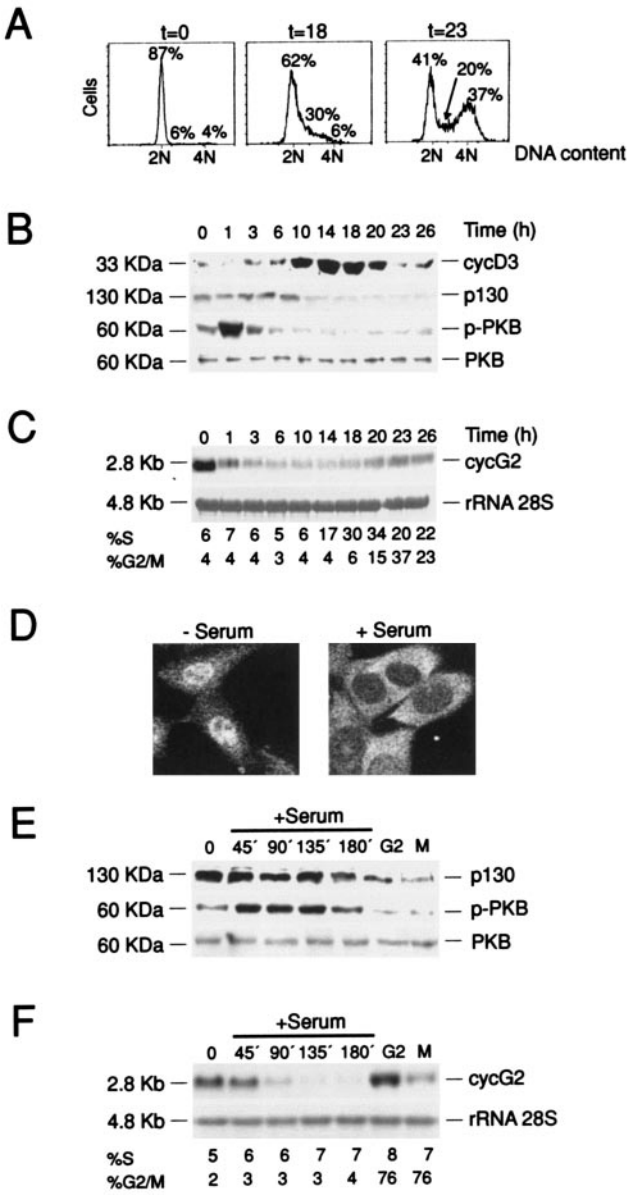

FIG. 1. Cyclin G2 mRNA levels are maximal in G_0. (A to C) NIH 3T3 cells were arrested by confluence and then released by low-density replating in medium with serum for different time periods. (A) Representative cell cycle profiles of cells 0, 18, and 23 h after release, showing the percentage of cells in G_0/G_1, S, and G_2/M. (B) Western blot analysis of the NIH 3T3 cells entering the cell cycle synchronously, using anti-cyclin D3 (cycD3), anti-p130, anti-phospho Ser 473-PKB (pPKB), or anti-PKB antibody. (C) Northern blot analysis of cyclin G2 expression. Total RNA was extracted from NIH 3T3 cells (same as in panels A and B), resolved in agarose gels (10 μg), transferred, and hybridized with a probe for cyclin G2 or 28S rRNA. The percentage of cells in the S and G_2/M phases is indicated. (D) Representative FKHRL1 (FoxO3a) immunofluorescence staining of NIH 3T3 cells deprived of serum for 18 h (−serum) or deprived of serum for 18 h and then incubated with serum for 1 h (+serum). (E and F) NIH 3T3 cells deprived of serum for 18 h (time 0), deprived of serum for 18 h and then incubated with serum for different times (indicated in minutes), or arrested in the G_2 or M phase. (E) Western blot analysis using the indicated antibodies. (F) Northern blot analysis of cyclin G2 expression. Total RNA was extracted from aliquots of the cells used in panel E. The percentage of cells in the S and G_2/M phases is indicated. The figure illustrates a representative experiment of at least three with similar results.

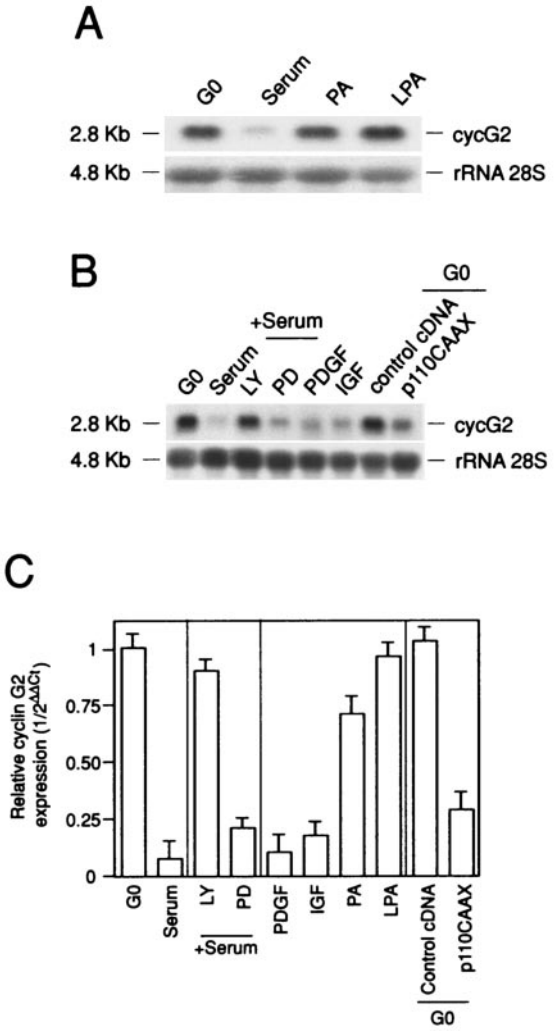

FIG. 2. Downregulation of cyclin G2 mRNA levels in G_1 requires PI3K activation. (A and B) Northern blot analysis for cyclin G2 expression in total RNA from NIH 3T3 cells incubated with different stimuli. (A) Cells were G_0 arrested and stimulated (3 h) with 10% serum, 10-ng/ml LPA, or 100 μM PA. (B) Cells were G_0 arrested and stimulated (3 h) with 15-ng/ml PDGF or 20-ng/ml IGF. Other samples were preincubated (1 h) with 10 μM LY294002 (LY) or 2 μM PD98059 (PD) and subsequently treated with 10% serum (3 h). Other samples were transfected with control cDNA or a vector encoding p110-CAAX (indicated); after incubation (8 h) in medium with serum, cells were cultured in the absence of serum for 18 h (G_0) prior to analysis. (C) Q-PCR analysis of cyclin G2 expression. cDNA was obtained from cells treated as in panels A and B. For each condition, the amount of cyclin G2 cDNA relative to that of actin was estimated according to the Ct, which defines the PCR cycle number at which the signal reaches a defined value. The relative amount of cyclin G2 was calculated according to the formula $\Delta Ct_{\text{cyclin G2}} = Ct_{\text{cyclin G2}} - Ct_{\text{actin}}$. Because maximal cyclin G2 expression is found in G_0, relative expression under the different conditions (x) was compared to that of G_0 by using the formula $\Delta\Delta Ct = \Delta Ct_{\text{cyclin G2}}\ (G_0) - \Delta Ct_{\text{cyclin G2}}\ (x)$. The mean ± standard deviation of three experiments is shown.

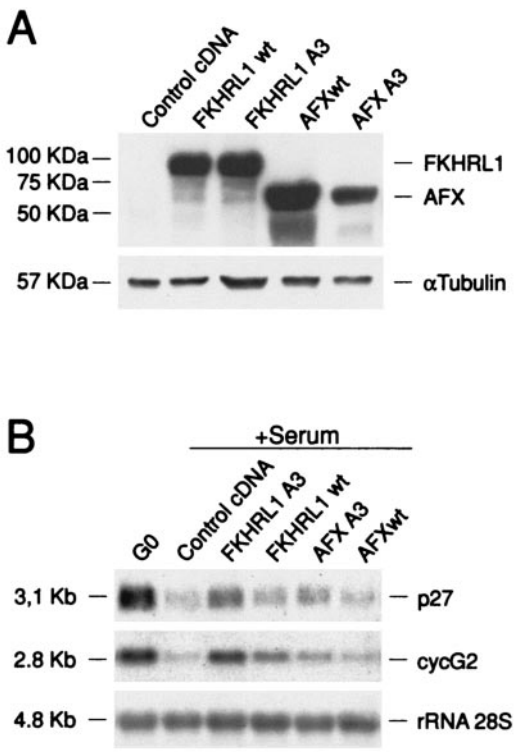

FIG. 3. Activation of FoxO genes induces cyclin G2 mRNA expression. (A and B) NIH 3T3 cells were transfected with cDNA encoding FoxO3a wt (HA-FKHRL1) or active forms (HA-FKHRL1A3) or FoxO4 wt (HA-AFX) or active forms (HA-AFXA3). (A) Expression of FoxO TFs was examined by Western blotting with an anti-HA antibody. α-Tubulin expression was used as a control for equivalent loading. (B) After transfection, a fraction of the cells (same as in panel A) were incubated (8 h) in medium with serum, starved for 18 h in serum-free medium, and then examined (G_0) or incubated (3 h) with 10% serum prior to analysis. Cell lysates were analyzed by Northern blotting with probes specific for $p27^{kip}$, cyclin G2, or 28S rRNA.

one of the most abundant serum components (48), or were incubated with PA, a mitogenic compound found in serum (16). Whereas serum induces a dramatic reduction in cyclin G2 mRNA levels, neither LPA nor PA mediated this effect (Fig. 2A). Serum also contains growth factors such as PDGF and IGF1; incubation with either of these reduced cyclin G2 mRNA levels (Fig. 2B). Small molecule inhibitory drugs were used to determine whether activation of the PI3K or mitogen-activated protein kinase (MAPK) pathways, downstream of these Tyr kinase growth factor receptors, was involved in triggering cyclin G2 mRNA downregulation. The MAPK inhibitor PD98059 blocked serum-induced MAPK phosphorylation (not shown), but did not affect cyclin G2 mRNA downregulation (Fig. 2B). In contrast, incubation with the PI3K inhibitor LY294002 (Fig. 2B) or wortmannin (data not shown) significantly blocked serum-induced cyclin G2 downregulation. To mimic PI3K activation in the absence of serum, cells were transfected with a recombinant membrane-tagged form of the p110α catalytic subunit (p110-CAAX) (25, 26). p110-CAAX expression resulted in moderate downregulation of cyclin G2 mRNA levels, which was not as large as that mediated by PDGF, IGF, or serum (Fig. 2B). Similar results were obtained by quantitative PCR (Fig. 2C). These results suggest that PI3K activation is necessary but not sufficient for the downregulation of cyclin G2 mRNA expression observed in G_1.

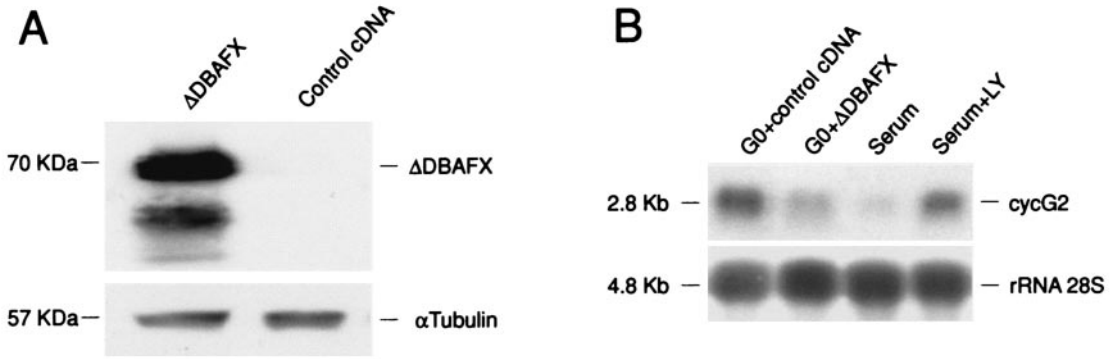

FIG. 4. Interfering mutants of FoxO genes downregulate cyclin G2 mRNA expression in G_0. NIH 3T3 cells were transiently transfected with a control vector or with HA-ΔDBAFX. (A) Cells were cultured for 24 h. HA-ΔDBAFX expression was examined by Western blotting with an anti-HA antibody. α-Tubulin expression was analyzed as a loading control. (B) After transfection, a fraction of the cells (same as in panel A) were incubated (8 h) in medium with serum and then were cultured in the absence of serum for 18 h (G_0) and then collected and examined. Untransfected control cells were cultured in the absence of serum (18 h) and then incubated with serum (3 h) or preincubated with LY294002 (1 h) prior to serum treatment (3 h). Total RNA was examined by Northern blot analysis for cyclin G2 mRNA expression relative to 28S rRNA levels. A representative experiment is shown of three experiments performed with similar results.

FoxO3a activates cyclin G2 mRNA expression. To examine the mechanisms by which PI3K activation mediates a reduction in cyclin G2 mRNA levels, we considered that the PI3K-PKB pathway inhibits FoxO TF activity (4, 7, 11, 19, 29, 30, 47) and postulated that FoxO TF may regulate cyclin G2 expression. The expression profiles of cyclin G2 mRNA (Fig. 1) correlate with FoxO TF activity during the cell cycle, which is high in quiescent and in G_2-phase cells (2).

To examine whether FoxO TFs control cyclin G2 mRNA expression, NIH 3T3 cells were transfected with FKHRL1 (FoxO3a); its active version, FKHRL1A3 (6); or AFX (FoxO4) or its active version, AFXA3 (30) (Fig. 3A). We tested transcriptional activity of AFX and FKHRL1 by examining $p27^{kip}$ mRNA expression, which was high in G_0 and decreased after serum addition (Fig. 3B). AFXA3 expression and, even more clearly, FKHRL1A3 expression mediated a $p27^{kip}$ expression increase in G_1 (Fig. 3B). We then examined cyclin G2 mRNA levels: AFX, AFXA3, and FKHRL1 expression increased cyclin G2 mRNA levels moderately, whereas FKHRL1A3 significantly enhanced cyclin G2 mRNA expression in G_1 (Fig. 3B).

We also tested whether disruption of endogenous FoxO TF action (2) affects cyclin G2 expression. NIH 3T3 cells expressing the ΔDBAFX dominant-negative mutant (2, 30) (Fig. 4A) were arrested in G_0, and cyclin G2 mRNA levels were examined (Fig. 4B). As a control, cyclin G2 expression was examined in parallel in the G_0 and G_1 phases (Fig. 4B). Interference with endogenous FoxO TF action by ΔDBAFX expression significantly reduced cyclin G2 mRNA levels in G_0 (Fig. 4B). Similar results were obtained by Q-PCR (data not shown).

Cyclin G2 promoter binds and is transactivated by FoxO3a. We examined the murine cyclin G2 promoter (23) and found FoxO TF consensus binding site motifs (6, 62) (Fig. 5A). Electrophoretic mobility shift assays were used to examine whether FoxO TFs bind to these FoxO consensus binding sites in the cyclin G2 promoter. We first tested whether nuclear proteins from the control Burkitt's lymphoma cell line DG75 bind to the clustered FoxO elements of the cyclin G2 promoter. Radiolabeled FoxO-cyclin G2 oligonucleotides (bp −1296 to −1266) formed complexes with proteins from DG75 nuclear extracts (Fig. 5B). These complexes were displaced not only by the FoxO cyclin G2 element, but also by a FoxO consensus motif (61) (Fig. 5C). Nuclear extracts of NIH 3T3 cells in different cell cycle phases were assayed with the FoxO cyclin G2 probe, showing increased complex formation using G_0- and G_2-phase cell extracts compared to extracts from G_1-phase cells (Fig. 5D). Complex formation was efficiently dissociated by an excess of either the unlabeled FoxO cyclin G2 element or the FoxO consensus oligonucleotides (Fig. 5D). Moreover, the FKHRL1 (FoxO3a) antibody, but not the control anti-DP1 antibody, was able to supershift these complexes, showing that FoxO3a binds to the FoxO TF motifs in the cyclin G2 promoter (Fig. 5D).

FoxO3a association with the cyclin G2 promoter in vivo was also examined by ChIP assays using G_2-arrested cells. Immunoprecipitation of chromatin with anti-FKHRL1 (FoxO3a) antibody and subsequent PCR analysis of the associated DNA showed association of FKHRL1 (FoxO3a) with the cyclin G2 promoter region encompassing the FoxO motifs (illustrated in Fig. 5A) (Fig. 6A). As a negative control, the cyclin D3 promoter was tested in parallel, showing that the cyclin D3 promoter does not associate with FKHRL1 TF (Fig. 6A). In conclusion, our data support a model whereby FoxO TF regulates cyclin G2 expression by direct binding to the cyclin G2 promoter.

To assess the influence of FoxO TF binding to its elements within the cyclin G2 promoter, the region containing the FoxO TF motifs (in Fig. 5A) was inserted upstream of a basal promoter controlling luciferase expression. Cotransfection of these constructs with AFXA3 or FKHRL1A3, but not with ΔDBAFX, induced an increase in reporter expression (Fig. 6B), within the range of previously described FoxO-controlled promoters (2, 6, 34). FKHRL1 also transactivated the FasL promoter (2, 6), but not the myc promoter (2, 56) (Fig. 6B).

DISCUSSION

Cyclin G2 is a member of the G-type cyclins and is expressed in various amounts during the cell cycle in lymphocytes (20,

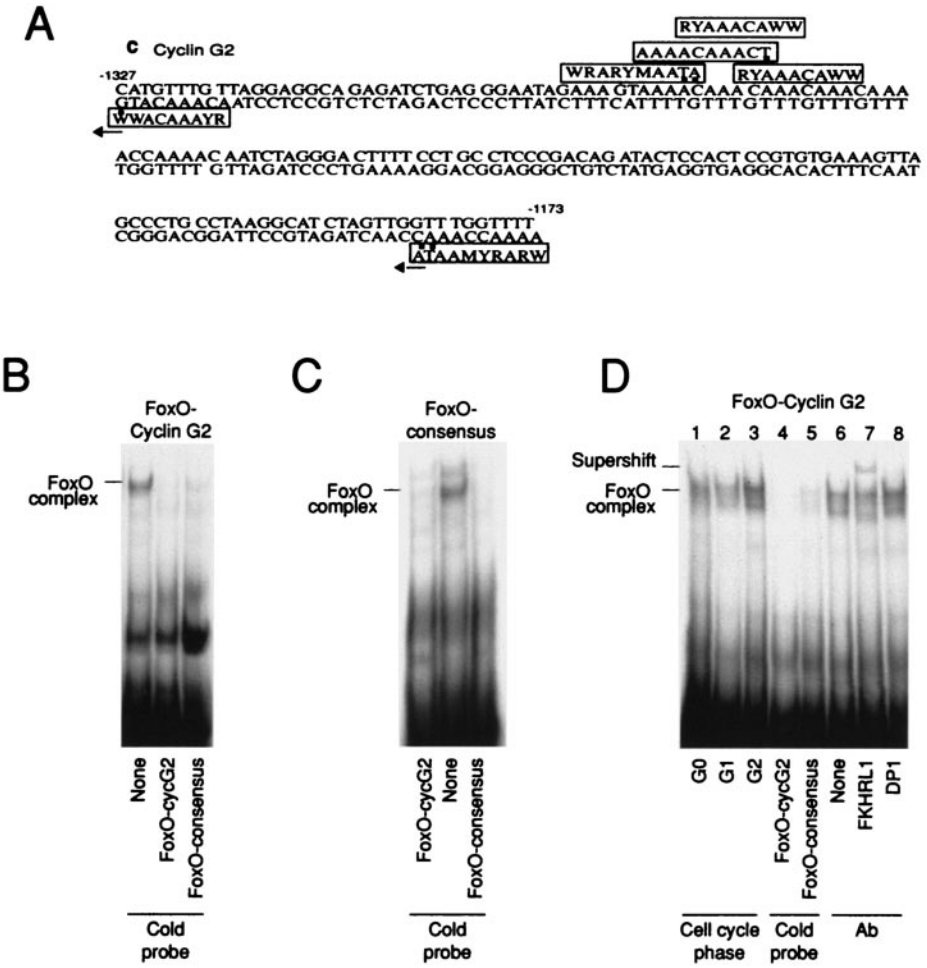

FIG. 5. FoxO transcription factors bind to the cyclin G2 promoter. (A) Murine cyclin G2 promoter region containing the following FoxO TF consensus motifs: FKH1 consensus RYAAACAWW, *Xenopus* FKH consensus WRARYMAATA, IGFBP1 FKH-responsive promoter element AAAACAAACT (R = A/G, Y = T/C, W = A/T, M = A/C, K = T/G). Black dots indicate mismatches. Numbers indicate the position in the promoter relative to the transcription initiation site. (B and C) Electrophoretic mobility shift assays were performed with DG75 nuclear extracts and radiolabeled oligonucleotides representing the clustered FoxO consensus binding sites in the cyclin G2 promoter (FoxO-cycG2) (B) or a previously described FoxO consensus probe (C) (61). Reaction mixtures were preincubated alone (None) or with a 100-fold excess of the unlabeled competitor oligonucleotides (B and C [cold probe indicated]). (D) NIH 3T3 cells were arrested at different cell cycle phases, and complexes formed by incubating nuclear extracts with radiolabeled FoxO-cyclin G2 oligonucleotides were analyzed (lanes 1 to 3). Reaction mixtures prepared from G2-arrested NIH 3T3 cells were preincubated for 20 min prior to addition of labeled probes with a 100-fold excess of the unlabeled competitor oligonucleotides (cold probe, lanes 4 and 5), alone (lane 6), with anti-FKHRL1 antibody (lane 7), or with a control antibody (Ab) (anti-DP1, lane 8). A representative experiment is shown.

21). Ectopic expression of cyclin G2 inhibits cell cycle progression (3), suggesting that this protein acts as a cell cycle inhibitor. Here we studied the mechanisms that regulate cyclin G2 mRNA expression during the cell cycle. Using NIH 3T3 cells, we found elevated cyclin G2 mRNA expression levels in the G_0 phase, which decreased as cells entered the cell cycle. Downregulation of cyclin G2 mRNA in the G_1 phase requires PI3K-PKB activation. Since PI3K-PKB inhibits FoxO TFs, we postulated that these TFs may regulate cyclin G2 expression. Our findings show that FoxO TFs, negatively controlled by PI3K-PKB, regulate cyclin G2 expression during the cell cycle. These observations unmask a new role for PI3K-PKB and FoxO TFs in the control of cell cycle entry.

Several lines of evidence support FoxO TF control of cyclin G2 mRNA expression. The kinetics of cyclin G2 expression (Fig. 1) resembles those of FoxO TF activation (2). Expression of an active FoxO TF increased the normally low cyclin G2 mRNA levels in the G_1 phase, whereas interference with endogenous FoxO TF activity by expression of an inactive form reduces physiologically high cyclin G2 expression levels in quiescent cells. The cyclin G2 promoter contains clustered FoxO TF consensus motifs that bind and are transactivated by FoxO TFs. Finally, as shown by ChIP assays, endogenous FoxO TFs bind the cyclin G2 promoter in live cells.

Because these studies were performed with the murine cyclin G2 promoter, we also searched for FoxO TF consensus binding sites in the human promoter. Human and murine cyclin G2 promoters show several areas of significant similarity,

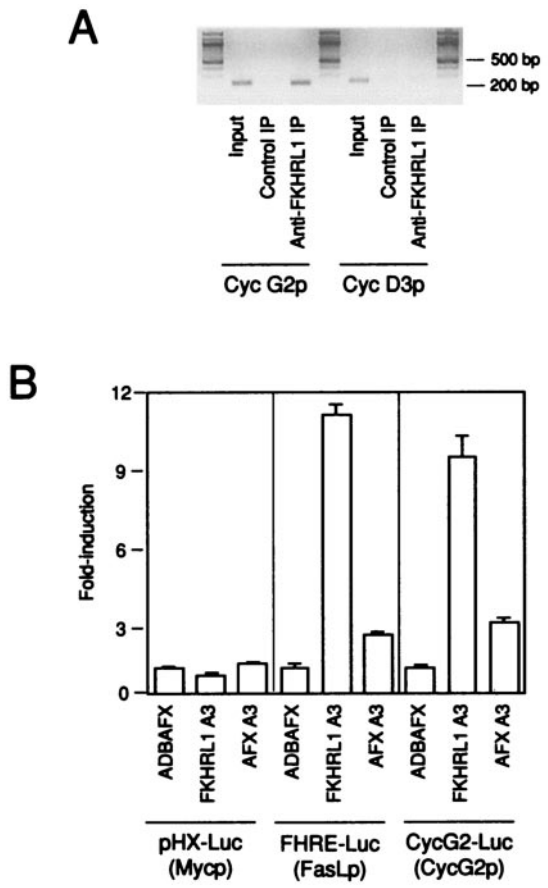

FIG. 6. FoxO genes transactivate the cyclin G2 promoter. (A) Chromatin suspensions from G_2-arrested NIH 3T3 cells were incubated with normal rabbit serum (control immunoprecipitation [IP]) or with an anti-FKHRL1 antibody. DNA was eluted from the control or FKHRL1 IP and tested by PCR with oligonucleotides flanking the cyclin G2 promoter region described in the legend to Fig. 5A or with a region of the cyclin D3 promoter as a control. Total chromatin extracts were examined by PCR as positive controls (input). (B) NIH 3T3 cells were cotransfected with luciferase reporter plasmids as indicated and with HA-FKHRL1A3, HA-AFXA3, or HA-ΔDBAFX; luciferase activity was measured (light units). Background signals for cells cotransfected with luciferase plasmids and a control empty vector were subtracted from each sample. The *y* axis shows the *x*-fold induction of luciferase activity for reporter plasmids cotransfected with HA-FKHRL1A3 or HA-AFXA3 relative to the luciferase activity of reporter plasmids cotransfected with inactive FoxO (HA-ΔDBAFX). The mean ± standard deviation of three independent experiments is shown. Mycp, *MYC* promoter; FasLp, Fas ligand promoter; CycG2p, cyclin G2 promoter.

according to the Blast 2 sequence program. One of these regions, which contains several clustered forkhead consensus binding sites in the murine promoter (Fig. 5A), also contains clustered forkhead motifs in the human promoter. The clustered consensus motifs of the murine promoter (AF079877) are at positions −1296 to −1266 from the translation initiation site (included in Fig. 5A), whereas in the human gene (AF549495), the clustered forkhead motifs are at positions −1470 to −1440, with two additional sites in the 100-bp surrounding area (data not shown), as in the murine promoter (Fig. 5A).

PI3K-PKB activation, which inactivates FoxO TFs (6, 14, 31), was found to be necessary for cyclin G2 downregulation during cell cycle entry. Despite the necessity for PI3K activation to downregulate cyclin G2 synthesis, expression of an active PI3K form in quiescent cells was insufficient to decrease cyclin G2 expression to the levels observed following serum-induced cell cycle entry. This suggests that signals in addition to PI3K activation mediate cyclin G2 downregulation during the G_1 phase. Because FoxO TFs are also inactivated by Ral pathways (12), Ral activation in G_1 may contribute to decreasing cyclin G2 expression. In addition, mechanisms other than those mediated by FoxO TFs may contribute to regulating cyclin G2 transcription. In support of this hypothesis, interfering forms of FoxO genes reduce, but do not abrogate, cyclin G2 expression. We previously reported that the transcriptional activity of FoxO TFs in the G_2 phase regulates expression of cyclin B and polo-like kinase (2), which are also regulated by other TFs (9). Because cells require different genetic programs for these phases, it is likely that other TFs selectively expressed in G_0 or G_2 modulate expression of the FoxO gene targets in the G_0 and G_2 phases.

We show that cyclin G2 expression is high in G_0, decreases as cells enter the cell cycle, and increases again in the late S and G_2 phases. The G_0 phase, a state of cellular quiescence, is characterized by low protein synthesis activity (1), as well as by high p130 and $p27^{kip}$ protein levels, low cyclin D levels, inactivation of the PI3K-PKB pathway, and activation or nuclear localization of FoxO TFs (2, 4, 22, 33, 51, 54). In contrast, the G_1 phase is characterized by high protein synthesis levels (1) and by activation of G_1-type cyclins or Cdks (22, 51). Rapid, transient activation of PI3K-PKB and inactivation of FoxO TF are also observed following growth factor receptor stimulation (2), followed by a gradual decrease in p130 (54) and $p27^{kip}$ (33) and an increase in G_1-phase cyclins (22, 51). Here, G_0 cells were obtained either by serum deprivation or, alternatively, by growth to confluence, which is considered more physiological. Both approaches yielded cells with a G_0 phenotype, according to the criteria described above. Serum depletion was nonetheless more efficient at inducing FoxO TF cytosolic exclusion (Fig. 1D) than growth to confluence, because in more than 90% of confluent cells, FKHRL1 (FoxO3a) was distributed between nuclei and cytosol (data not shown). The distinct intracellular localization of FKHRL1 induced by the two techniques suggests that these methods generate qualitatively different quiescent states, as previously suggested (reviewed in reference 10). Nonetheless, dual nuclear and cytosolic localization, correlating with the presence of active FoxO TFs, was previously described in G_2-phase cells (2). To examine cyclin G2 fluctuation during the cell cycle, we also performed kinetic studies of cells at different times after release from quiescence. In this protocol, a significant proportion of cells progress through the cell cycle in parallel (Fig. 1A), validating the use of this approach to examine gene expression during cell cycle progression. Despite the limitations of these techniques, the criteria used to differentiate the G_0 and G_1 phases support cyclin G2 expression in G_0. Moreover, in cells released from quiescence, cyclin G2 expression decreased in the first 1 to 2 h after serum addition, indicating that cyclin G2 expression decreases in the G_1 phase, since the following phase, S phase, does not began until 16 to 18 h after serum addition, as deter-

mined by DNA synthesis analysis. Cyclin G2 expression in the G_2 phase was confirmed by using cells arrested in the G_2 phase.

Previous reports showed variation in cyclin G2 expression levels during the cell cycle in lymphocytes (20, 21); its fluctuation in distinct cell types thus suggests a broader role for cyclin G2 as a cell cycle inhibitor. Using T lymphoblasts and Jurkat cells, Horne et al. reported that the highest cyclin G2 mRNA levels are found in the S phase (21), although the S-phase-enriched fractions examined contained G_2-phase cells. They also observed high cyclin G2 content in a G_0/G_1-phase cell fraction (21), although DNA content measurement, used to examine cell cycle phases, did not allow discrimination between G_0 and G_1 phases. Overexpression of cyclin G2 was found to inhibit cell cycle progression (G_0/G_1- to S-phase transition) (3), but the reported data do not permit us to distinguish between a G_0 or G_1 arrest. Cyclin G2 involvement in quiescence maintenance, nonetheless, concurs with the observation of high cyclin G2 expression levels in terminally differentiated cells (21).

Cell cycle progression is a tightly controlled process. To initiate cell division, mitogens trigger a number of early signals that induce cell growth and activation of cyclin D/cdk4 or cyclin D/cdk6, which is followed by cyclin E expression and cdk2 activation, events required to trigger DNA synthesis (22, 51, 52). Among the early signals induced by growth factor receptor stimulation, PI3K activation is essential for cell cycle entry (2, 28, 29, 34). PI3K activity governs cell growth and cyclin D levels (13, 28), events essential for progression through the G_1 phase. In addition, PI3K-PKB controls inactivation of FoxO TF, which in turn regulates expression of the cyclin E/cdk2 inhibitor $p27^{kip}$ and p130 (31, 34). However, the contribution of p130 in quiescence is unclear (31, 54), and $p27^{kip}$ acts as an inhibitor of S-phase entry (52). The observation that FoxO TFs, and specifically FoxO3a, induce cyclin G2 expression in G_0 therefore indicates a mechanism by which these TFs contribute to quiescence maintenance. Inhibition of cyclin G2 expression by PI3K-PKB activation illustrates a new role for PI3K in mediating G_0/G_1 transition.

Our observations support biphasic, complementary regulation of FoxO TFs and PI3K during the cell cycle. PI3K is inactive in G_0, whereas FoxO TFs are active and induce synthesis of cyclin G2. In G_1, PI3K-PKB is turned on and inactivates FoxO TF, which induces downregulation of cyclin G2 expression. Finally, in G_2, PI3K is inactive; FoxO TF is again activated and is necessary for cell cycle termination (2) and cyclin G2 synthesis, which may also facilitate cell cycle exit.

ACKNOWLEDGMENTS

We thank M. E. Greenberg and K. Sugamura for vectors, B. Alvarez for advice in ChIP assays, I. Molina for DG75 nuclear extracts, J. A. Garcia-Sanz for help with Northern blots, A. Zaballos for help with Q-PCR, and C. Mark for editorial assistance.

This work was supported by grants from the European Union (QLRT-2001-02171), the Community of Madrid (08.3/0030), and the Spanish Ministry of Science and Technology (SAF2001-2278 and BMC2001-1738). The Department of Immunology and Oncology was founded and is supported by the Spanish Council for Scientific Research (CSIC) and by Pfizer.

REFERENCES

1. **Alvarez, B., E. Garrido, J. A. Garcia-Sanz, and A. C. Carrera.** 2003. Phosphoinositide 3-kinase activation regulates cell division time by coordinated control of cell mass and cell cycle progression rate. J. Biol. Chem. **27:**26466–26473.
2. **Alvarez, B., C. Martinez-A., B. M. T. Burgering, and A. C. Carrera.** 2001. Forkhead transcription factors contribute to execution of the mitotic programme in mammals. Nature **413:**744–747.
3. **Bennin, D. A., A. S. Don, T. Brake, J. L. McKenzie, H. Rosenbaum, L. Ortiz, A. A. DePaoli-Roach, and M. C. Horne.** 2002. Cyclin G2 associates with protein phosphatase 2A catalytic and regulatory B′ subunits in active complexes and induces nuclear aberrations and a G1/S phase cell cycle arrest. J. Biol. Chem. **277:**27449–27467.
4. **Biggs, W. H. I., J. Meisenhelder, T. Hunter, W. K. Cavenee, and K. C. Arden.** 1999. Protein kinase B/Akt-mediated phosphorylation promotes nuclear exclusion of the winged helix transcription factor FKHR1. Proc. Natl. Acad. Sci. USA **96:**7421–7426.
5. **Boyd, K. E., J. Wells, J. Gutman, S. M. Bartley, and P. J. Farnham.** 1998. c-Myc target gene specificity is determined by a post-DNA binding mechanism. Proc. Natl. Acad. Sci. USA **95:**13887–13892.
6. **Brunet, A., A. Bonni, M. J. Zigmond, M. Z. Lin, P. Juo, L. S. Hu, M. J. Anderson, K. C. Arden, J. Blenis, and M. E. Greenberg.** 1999. Akt promotes cell survival by phosphorylating and inhibiting a Forkhead transcription factor. Cell **96:**857–868.
7. **Burgering, B. M., and G. J. Kops.** 2002. Cell cycle and death control: long live Forkheads. Trends Biochem. Sci. **7:**352–360.
8. **Campanero, M. R., M. Armstrong, and E. Flemington.** 1999. Distinct cellular factors regulate the c-*myb* promoter through its E2F element. Mol. Cell. Biol. **19:**8442–8450.
9. **Cogswell, J. P., M. M. Godlevski, M. Bonham, J. Bisi, and L. Babiss.** 1995. Upstream stimulatory factor regulates expression of the cell cycle-dependent cyclin B1 gene promoter. Mol. Cell. Biol. **15:**2782–2790.
10. **Cooper, S.** 2003. Reappraisal of serum starvation, the restriction point, G0, and G1 phase arrest points. FASEB J. **17:**333–340.
11. **del Peso, L., V. M. Gonzalez, R. Hernandez, F. G. Barr, and G. Nunez.** 1999. Regulation of the forkhead transcription factor FKHR, but not the PAX3-FKHR fusion protein, by the serine/threonine kinase Akt. Oncogene **18:**7328–7333.
12. **De Ruiter, N. D., B. M. T. Burgering, and J. L. Bos.** 2001. Regulation of the Forkhead transcription factor AFX by Ral-dependent phosphorylation of threonines 447 and 451. Mol. Cell. Biol. **21:**8225–8235.
13. **Diehl, J. A., M. Cheng, M. F. Roussel, and C. J. Sherr.** 1998. Glycogen synthase kinase-3 beta regulates cyclin D1 proteolysis and subcellular localization. Genes Dev. **12:**3499–3511.
14. **Dijkers, P. F., R. H. Medema, J. W. Lammers, L. Koenderman, and P. J. Coffer.** 2000. Expression of the pro-apoptotic Bcl-2 family member Bim is regulated by the forkhead transcription FKHR-L1. Curr. Biol. **10:**1201–1204.
15. **Dynlacht, B. D.** 1997. Regulation of transcription by proteins that control the cell cycle. Nature **389:**149–152.
16. **Fang, Y., M. Vilella-Bach, R. Bachmann, A. Flanigan, and J. Chen.** 2001. Phosphatidic acid-mediated mitogenic activation of mTOR signaling. Science **294:**1942–1945.
17. **Fruman, D. A., R. E. Meyers, and L. A. Cantley.** 1998. Phosphoinositide kinases. Annu. Rev. Biochem. **67:**481–507.
18. **Furuyama, T., T. Nakazawa, I. Nakano, and N. Mori.** 2000. Identification of the differential distribution patterns of mRNAs and consensus binding sequences for mouse DAF-16 homologues. Biochem. J. **349:**629–634.
19. **Guo, S., G. Rena, S. Cichy, X. He, P. Cohen, and T. Unterman.** 1999. Phosphorylation of serine 256 by protein kinase B disrupts transactivation by FKHR and mediates effects of insulin on insulin-like growth factor-binding protein-1 promoter activity through a conserved insulin response sequence. J. Biol. Chem. **274:**17184–17192.
20. **Horne, M. C., K. L. Donaldson, G. L. Goolsby, D. Tran, M. Mulheisen, J. W. Hell, and A. F. Wahl.** 1997. Cyclin G2 is up-regulated during growth inhibition and B cell antigen receptor-mediated cell cycle arrest. J. Biol. Chem. **272:**12650–12661.
21. **Horne, M. C., G. L. Goolsby, K. L. Donaldson, D. Tran, M. Neubauer, and A. F. Wahl.** 1996. Cyclin G1 and cyclin G2 comprise a new family of cyclins with contrasting tissue-specific and cell cycle-regulated expression. J. Biol. Chem. **271:**6050–6061.
22. **Hunt, T.** 1991. Cyclins and their partners: from a simple idea to complicated reality. Semin. Cell Biol. **2:**213–222.
23. **Jensen, M. R., T. Audolfsson, C. L. Keck, D. B. Zimonjic, and S. S. Thorgeirsson.** 1999. Gene structure and chromosomal localization of mouse cyclin G2 (Ccng2). Gene (Amsterdam) **230:**171–180.
24. **Jensen, M. R., V. M. Factor, and S. S. Thorgeirsson.** 1998. Regulation of cyclin G1 during murine hepatic regeneration following Dipin-induced DNA damage. Hepatology **28:**537–546.
25. **Jimenez, C., D. R. Jones, P. Rodriguez-Viciana, A. Gonzalez-Garcia, E. Leonardo, S. Wennstrom, C. von Kobbe, J. L. Toran, L.-R. Borlado, V. Calvo, S. G. Copin, J. P. Albar, M. L. Gaspar, E. Diez, M. A. Marcos, J. Downward, C. Martinez-A., I. Merida, and A. C. Carrera.** 1998. Identification and characterization of a new oncogene derived from the regulatory subunit of phosphoinositide 3-kinase. EMBO J. **17:**743–753.
26. **Jimenez, C., R. A. Portela, M. Mellado, J. M. Rodriguez-Frade, J. Collard,**

A. Serrano, C. Martinez-A., J. Avila, and A. C. Carrera. 2000. Role of the PI3K regulatory subunit in the control of actin organization and cell migration. J. Cell Biol. **151:**249–262.
27. **Kaestner, K. H., W. Knochel, and D. E. Martinez.** 2000. Unified nomenclature for the winged helix/forkhead transcription factors. Genes Dev. **14:**142–146.
28. **Klippel, A., M.-A. Escobedo, M. S. Wachowicz, G. Apell, T. W. Brown, M. A. Giedlin, W. M. Kavanaugh, and L. T. Williams.** 1998. Activation of phosphatidylinositol 3-kinase is sufficient for cell cycle entry and promotes cellular changes characteristic of oncogenic transformation. Mol. Cell. Biol. **18:**5699–5711.
29. **Kops, G. J., and B. M. Burgering.** 2000. Forkhead transcription factors are targets of signalling by the proto-oncogene PKB (C-AKT). J. Anat. **197**(part 4)**:**571–574.
30. **Kops, G. J., N. D. de Ruiter, A. M. De Vries-Smits, D. R. Powell, J. L. Bos, and B. M. Burgering.** 1999. Direct control of the Forkhead transcription factor AFX by protein kinase B. Nature **398:**630–634.
31. **Kops, G. J. P. L., R. H. Medema, J. Glassford, M. A. G. Essers, P. F. Dijkers, P. J. Coffer, E. W.-F. Lam, and B. M. T. Burgering.** 2002. Control of cell cycle exit and entry by protein kinase B-regulated Forkhead transcription factors. Mol. Cell. Biol. **22:**2025–2036.
32. **Lew, J., and J. H. Wang.** 1995. Neuronal cdc2-like kinase. Trends Biochem. Sci. **20:**33–37.
33. **MacLachlan, T. K., N. Sang, and A. Giordano.** 1995. Cyclins, cyclin-dependent kinases and cdk inhibitors: implications in cell cycle control and cancer. Crit. Rev. Eukaryot. Gene Expr. **5:**127–156.
34. **Medema, R. H., G. J. Kops, J. L. Bos, and B. M. Burgering.** 2000. AFX-like Forkhead transcription factors mediate cell-cycle regulation by Ras and PKB through p27kip1. Nature **404:**782–787.
35. **Morgan, D. O.** 1997. Cyclin-dependent kinases: engines, clocks, and microprocessors. Annu. Rev. Cell Dev. Biol. **13:**261–291.
36. **Müllner, E. W., and J. A. Garcia-Sanz.** 1997. Analysis of RNA expression by Northern blotting, p. 401–424. *In* I. Lefkovits (ed.), Immunology methods manual, vol. 1. Academic Press, London, United Kingdom.
37. **Nakamura, T., R. Sanokawa, Y. F. Sasaki, D. Ayusawa, M. Oishi, and N. Mori.** 1995. Cyclin I: a new cyclin encoded by a gene isolated from human brain. Exp. Cell Res. **221:**534–542.
38. **Noble, M. E., J. A. Endicott, N. R. Brown, and L. N. Johnson.** 1997. The cyclin box fold: protein recognition in cell cycle and transcription control. Trends Biochem. Sci. **22:**482–487.
39. **Nugent, J. H., C. E. Alfa, T. Young, and J. S. Hyams.** 1991. Conserved structural motifs in cyclins identified by sequence analysis. J. Cell Sci. **99:**669–674.
40. **Ohshima, T., J. M. Ward, C. G. Huh, G. Longenecker, Veeranna, H. C. Pants, R. O. Brady, L. J. Martin, and A. B. Kulkarni.** 1996. Targeted disruption of the cyclin-dependent kinase 5 gene results in abnormal corticogenesis, neuronal pathology and perinatal death. Proc. Natl. Acad. Sci. USA **93:**11173–11178.
41. **Okamoto, K., C. Kamibayashi, M. Serrano, C. Prives, M. C. Mumby, and D. Beach.** 1996. p53-dependent association between cyclin G and the B′ subunit of protein phosphatase 2A. Mol. Cell. Biol. **16:**6593–6602.
42. **Pardee, A. B.** 1989. G1 events and regulation of cell proliferation. Science **246:**603–608.
43. **Pines, J.** 1995. Cyclins and cyclin-dependent kinases: a biochemical view. Biochem. J. **308:**697–711.
44. **Pines, J.** 1995. Cyclins and cyclin-dependent kinases: theme and variations. Adv. Cancer Res. **66:**181–212.
45. **Polyak, K., M. H. Lee, H. Erdjument-Bromage, A. Koff, J. M. Roberts, P. Tempst, and J. Massague.** 1994. Cloning of p27Kip1, a cyclin-dependent kinase inhibitor and a potential mediator of extracellular antimitogenic signals. Cell **78:**59–66.
46. **Polymenis, M., and E. V. Schmidt.** 1999. Coordination of cell growth with cell division. Curr. Opin. Genet. Dev. **9:**76–80.
47. **Rena, G., S. Guo, S. Cichy, T. G. Unterman, and P. Cohen.** 1999. Phosphorylation of the transcription factor forkhead family member FKHR by protein kinase B. J. Biol. Chem. **274:**17179–17183.
48. **Ridley, A. J., and A. Hall.** 1992. The small GTP-binding protein rac regulates growth factor-induced membrane ruffling. Cell **70:**389–399.
49. **Saucedo, L. J., and B. A. Edgar.** 2002. Why size matters: altering cell size. Curr. Opin. Genet. Dev. **12:**565–571.
50. **Schmidt, M., S. Fernandez de Mattos, A. van der Horst, R. Klompmaker, G. J. P. L. Kops, E. W.-F. Lam, B. M. T. Burgering, and R. H. Medema.** 2002. Cell cycle inhibition by FoxO Forkhead transcription factors involves downregulation of cyclin D. Mol. Cell. Biol. **22:**7842–7852.
51. **Sherr, C. J.** 1995. D-type cyclins. Trends Biochem. Sci. **20:**187–190.
52. **Sherr, C. J., and J. M. Roberts.** 1999. CDK inhibitors: positive and negative regulators of G1-phase progression. Genes Dev. **13:**1501–1512.
53. **Shimizu, A., J. Nishida, Y. Ueoka, K. Kato, T. Hachiya, Y. Kuriaki, and N. Wake.** 1998. Cyclin G contributes to G2/M arrest of cells in response to DNA damage. Biochem. Biophys. Res. Commun. **242:**529–533.
54. **Smith, E. J., G. Leone, J. DeGregori, L. Jakoi, and J. R. Nevins.** 1996. The accumulation of an E2F-p130 transcriptional repressor distinguishes a G_0 cell state from a G_1 cell state. Mol. Cell. Biol. **16:**6965–6976.
55. **Stephens, L. R., T. R. Jackson, and P. T. Hawkins.** 1993. Agonist-stimulated synthesis of phosphatidylinositol(3, 4, 5)-trisphosphate: a new intracellular signalling system? Biochim. Biophys. Acta **1179:**27–75.
56. **Takeshita, T., T. Arita, M. Higuchi, H. Asao, K. Endo, H. Kuroda, N. Tanaka, K. Murata, N. Ishii, and K. Sugamura.** 1997. STAM, signal transducing adaptor molecule, is associated with Janus kinases and involved in signaling for cell growth and c-myc induction. Immunity **6:**449–457.
57. **Tamura, K., Y. Kanaoka, S. Jinno, A. Nagata, Y. Ogiso, K. Shimizu, T. Hayakawa, H. Nojima, and H. Okayama.** 1993. Cyclin G: a new mammalian cyclin with homology to fission yeast Cig1. Oncogene **8:**2113–2118.
58. **Tapon, N., K. H. Moberg, and I. K. Hariharan.** 2001. The coupling of cell growth to the cell cycle. Curr. Opin. Cell Biol. **13:**731–737.
59. **Vanhaesebroeck, B., and M. D. Waterfield.** 1999. Signaling by distinct classes of phosphoinositide 3-kinases. Exp. Cell Res. **253:**239–254.
60. **Zetterberg, A., and O. Larsson.** 1985. Kinetic analysis of regulatory events in G1 leading to proliferation or quiescence of Swiss 3T3 cells. Proc. Natl. Acad. Sci. USA **82:**5365–5369.
61. **Zhang, X., L. Gan, H. Pan, S. Guo, X. He, S. T. Olson, A. Mesecar, S. Adam, and T. G. Unterman.** 2002. Phosphorylation of serine 256 suppresses transactivation by FKHR (FOXO1) by multiple mechanisms. Direct and indirect effects on nuclear/cytoplasmic shuttling and DNA binding. J. Biol. Chem. **277:**45276–45284.
62. **Zhu, G., P. T. Spellman, T. Volpe, P. O. Brown, D. Botstein, T. N. Davis, and B. Futcher.** 2000. Two yeast forkhead genes regulate the cell cycle and pseudohyphal growth. Nature **406:**90–94.
63. **Zvelebil, M. J., L. MacDougall, S. Leevers, S. Volinia, B. Vanhaesebroeck, I. Gout, G. Panayotou, J. Domin, R. Stein, F. Pages, H. Koga, K. Salim, J. Linacre, P. Das, C. Panaretou, R. Wetzler, and M. D. Waterfield.** 1996. Structural and functional diversity of phosphoinositide 3-kinases. Philos. Trans. R. Soc. Lond. B Biol. Sci. **351:**217–223.